



# Wireless Sensor Networks for Continuous Structural Health Monitoring of Historic Masonry Towers

Paolo Barsocchi, Gianni Bartoli, Michele Betti, Maria Girardi, Stefano Mammolito, Daniele Pellegrini & Giacomo Zini

To cite this article: Paolo Barsocchi, Gianni Bartoli, Michele Betti, Maria Girardi, Stefano Mammolito, Daniele Pellegrini & Giacomo Zini (2021) Wireless Sensor Networks for Continuous Structural Health Monitoring of Historic Masonry Towers, International Journal of Architectural Heritage, 15:1, 22-44, DOI: [10.1080/15583058.2020.1719229](https://doi.org/10.1080/15583058.2020.1719229)

To link to this article: <https://doi.org/10.1080/15583058.2020.1719229>



Published online: 17 Feb 2020.



Submit your article to this journal [↗](#)



Article views: 994



View related articles [↗](#)



View Crossmark data [↗](#)



Citing articles: 42 View citing articles [↗](#)



# Wireless Sensor Networks for Continuous Structural Health Monitoring of Historic Masonry Towers

Paolo Barsocchi <sup>a</sup>, Gianni Bartoli <sup>b</sup>, Michele Betti <sup>b</sup>, Maria Girardi <sup>a</sup>, Stefano Mammolito<sup>c</sup>,  
Daniele Pellegrini <sup>a</sup>, and Giacomo Zini <sup>b</sup>

<sup>a</sup>Institute of Information Science and Technologies "A. Faedo" (ISTI-CNR), National Research Council of Italy (CNR), Pisa, Italy; <sup>b</sup>Department of Civil and Environmental Engineering, University of Florence, Florence, Italy; <sup>c</sup>Engineering Italy Solutions S.r.l. (EIS), Cosenza, Italy

## ABSTRACT

The recent developments of micro-electro-mechanical systems and wireless sensor networks allow today the use of low-cost and small-size sensors for continuous monitoring of civil structures. Both these features are very important for the low impact of the sensor grid in heritage structures, ensuring a low-cost and sustainable dynamic monitoring system. Over the last 20 years the use of sensor networks for continuous monitoring has received a growing interest. Anyway, still numerous questions remain opened about the sensitivity of measurement devices, the optimization of number and positioning of sensors, the energy efficiency of the network, and the development of algorithms for real-time data analysis. This paper, based on the aforementioned motivations, discusses about a monitoring system made of micro-electro-mechanical sensors connected through a wireless network. The architecture of the wireless sensor network and the automatized procedure proposed for the continuous processing of the recorded signals are discussed and described with reference to an explicative masonry tower case study. It is believed that the proposed technologies can provide an economical and relatively non-invasive tool for real-time structural monitoring and that, moreover, the availability of large amounts of data from actual measurements can give effective information on the structural behaviour of historic constructions.

## ARTICLE HISTORY

Received 19 June 2019  
Accepted 17 January 2020

## KEYWORDS

Cultural heritage structures (CHS); dynamic monitoring; ICT; model updating; structural health monitoring (SHM); wireless sensors network (WSN)

## 1. Introduction

The periodic monitoring of ancient buildings is becoming an essential element in the preservation of Cultural Heritage structures (CHS). Many, in fact, are the events (with environmental and/or anthropic origin) that can compromise safety and stability of historic constructions: ageing of materials, degradation, earthquakes, environmental vibrations, etc. (Cavalagli et al. 2017; Cavalagli, Comanducci, and Ubertini 2018). They can be assessed with the help of a long-term monitoring system, which allows increasing and updating the knowledge level of monumental buildings and can moreover lead to reduction and optimization of the maintenance costs.

In recent years, monitoring protocols coupled with appropriate mathematical and numerical models gained an increasing importance in the field of preservation and conservation of historic constructions, as evidenced by the growing scientific literature and exemplary case studies on the subject. However, it is

worth noting that, despite such increasing interest, dynamic monitoring has not yet found in the national or international codes the same relevance as classical methods of local investigation, such as static monitoring or even sonic and ultrasonic tests. The Italian Guidelines (DPCM 2011), which paid attention to the monitoring of monumental buildings, limit the interest of these techniques primarily to the evaluation of the main frequencies and mode shapes, recognizing however that “*the control of certain parameters of the dynamic response can, in some cases, represent one of the possible elements for identifying a change in the construction.*” Despite the Structural Health Monitoring (SHM) framework (Sohn et al. 2004) has been introduced some decades ago and despite some novelties both in sensing technologies and data processing, the application to historic civil engineering structures is still subject of debate and innovation among the research community.

The application of SHM to CHS, if compared with new buildings, is even more challenging because of the

**CONTACT** Michele Betti  [michele.betti@unifi.it](mailto:michele.betti@unifi.it)  Department of Civil and Environmental Engineering, University of Florence, Via di Santa Marta, 3, Florence, Italy

## TOPICS

SHM of historic buildings; Innovative sensing technologies for SHM; Illustrative case-studies.

uniqueness of each monitored structure and the issues arising from the preservation needs which characterize this kind of buildings. Such constraints require the design of monitoring systems based on a reduced number of small size sensors, in order to assure a reduced impact on the structure. This is in fact a key aspect when dealing with the CHS in order to avoid the set-up of complex and invasive monitoring systems. As a consequence, data obtained through Ambient Vibration Tests (AVTs) will be not so accurate in terms of mode shapes, due to use of sparse sensor grids. Anyway, frequencies and damping ratios can be estimated with a high degree of accuracy, as shown in the automated procedures for the Modal Parameters Identification (MPI) recently proposed by several authors (Cabboi et al. 2017; Neu et al. 2017; Rainieri and Fabbrocino 2015; Reynders, Houbrechts, and De Roeck 2012; Ubertini, Gentile, and Materazzi 2013).

Assuming that damage will alter the modal properties of a system, several damage sensitive properties (Dessi and Camerlengo 2015; Salawu 1997; Sinou 2009) have been investigated from the Eighties by means of AVTs. The proper choice of the sensor grid depends on both the properties of the investigated structures and the level of damage that should be potentially assessed. In the case of CHS, eigenfrequencies are still the reference property monitored to detect anomalies in the structural behaviour. Different authors (Cavalagli et al. 2017; Ubertini et al. 2016) show that a frequency shift can reveal the presence of damage in the CH buildings.

On the other hand, frequencies are strongly dependent on the environmental conditions such as temperature, humidity and, in some cases, wind speed. Ubertini et al. (2017) clearly showed the effects of temperature on the modal properties of the San Pietro bell-tower in Perugia. The increase of temperature led to a quite linear increase in the frequencies for the bending modes, while a negative correlation was found for the torsional modes with a decrease of the frequency with temperature. An exception to this behaviour was found in the freezing days, during which the frequency tended to increase with the decrease of temperature. This last result is explained by the authors with the volumetric expansion of the water absorbed by the mortar joints that, due to the freezing effect, leads to the stiffening of the masonry walls. Gentile, Guidobaldi, and Saisi (2016) investigated the correlation between the identified frequencies and the temperature through the analysis of the data collected during a one-year monitoring of the Gabbia tower in Mantua. The results show a positive linear correlation between frequency and temperature both for the bending and the torsional modes. Azzara et al. (2018) investigated the

temperature effects on the San Frediano bell-tower in Lucca, finding a positive correlation between frequency and temperature of all the identified modes, while in Azzara et al. (2019), the authors detected the effects of freezing on the natural frequencies of the Clock Tower in Lucca. Ramos et al. (2010) investigated the effects of the humidity on the Mogodouro clock tower and underlined the trend of the frequencies during the heavy rain period. With respect to the wind speed effects, there are still few researches in the field of historic constructions, but some results can be found in the AVTs data analysis collected on tall buildings. Wu et al. (2017) analysed the correlation between the recorded wind speed and the frequencies extracted from the monitoring data of a tall concrete building. The results underline a negative correlation between all the frequencies and the wind speed values.

To detect in the data any anomaly that could be correlated to the presence of damage, suitable statistical methods are used to remove the environmental effects, such as the Principal Components Analysis (PCA), the Multiple Data Regression and the Kernel PCA (Azzara et al. 2018; Rizzo et al. 2017; Ubertini et al. 2017). Among the monitoring system protocols proposed by the scholars in the last years, the Continuous Vibration-Based Structural Health Monitoring (CVB-SHM), based on automated procedures for MPI, seems to be a promising tool for the structural health monitoring of historic structures (Pecorelli, Ceravolo, and Epicoco 2018). In case of different levels of random excitation, the collection of quasi-continuous time histories allows the recognition of the lowest energy level of input necessary to the model identification of the system. Nevertheless, the wireless sensor network (WSN) technologies are not still widely applied for the CVB-SHM, apart from a few examples (Clementi et al. 2018; Potenza et al. 2015; Zonta et al. 2010).

This paper illustrates the design and application of a WSN for CVB-SHM purposes on a historic masonry tower. The whole system was designed within the framework of the MOSCARDÒ (*“Information and Communication Technologies for structural monitoring of ancient constructions based on wireless sensor networks and drones”*) research project, funded by the Region of Tuscany and spanning from 2016 to 2018. It was recently tested on few illustrative case studies of cultural heritage structures. The paper discusses on the capability of the designed monitoring system to identify the modal parameters with low-cost and little invasive devices, addressing to the main requirements for the SHM of CHS. The first section describes the sensor network and reports on its properties. Subsequently, the case study (a historic masonry tower in Livorno, Italy) is introduced and an automated algorithm for the

extraction of the structure's modal parameters is illustrated: the first 12 months of data collected by the WSN are shown and discussed with pros and cons. Finally, the last part of the paper focuses on the influence of the environmental parameters on the identified modal properties.

## 2. Wireless monitoring system design

Wireless Sensor Networks applications for structural health monitoring are relatively recent. In the field of cultural heritage, WSN have been used until now for mainly monitoring large archaeological excavations (Barlindhaug, Holm-Olsen, and Tømmervik 2007) or some environmental parameters within museums or historic buildings. To date, applications of WSN technology to structural monitoring of ancient buildings are still in experimental phase and are limited to prototypes and few research projects. One of these is the “SMooHS-Smart Monitoring of Historic Structures” (SMooHS 2011), an international and multidisciplinary research project aimed at developing an intelligent monitoring system for controlling the degradation processes of a cultural asset, and providing indications of possible critical situations. Another research project in the field is “HHMS-Historical Heritage Management System” (Zonta, Pozzi, and Zanon 2008; Zonta et al. 2010) where a framework for real-time monitoring and risk assessment of historic buildings is developed and tested with respect to an illustrative case study: the “*Porta Aquila*” (Eagle Gate), one of the main historical monuments in the town of Trento (Italy). HHMS is a framework based on an on-line internet-based platform for storing and managing data collected via a low-cost distributed sensing technology (accelerometers, strain gauges, thermometers, etc.) network. Another prototype is described in Barsocchi et al. (2018), where the bell-tower of the San Frediano church in Lucca was monitored. The authors deployed some Internet of Thing (IoT) sensor devices (MEMS accelerometers) on the San Frediano bell-tower and monitored the ambient vibrations of the structure for 6 months.

In general, despite the above-mentioned experiences, it can be stated that the dynamic monitoring of historic constructions via WSN is still developed as an episodic experimental activity. At the same time, the above-mentioned researches demonstrate that this framework can find, not interfering with the normal use of the structure and being totally non-invasive and completely reversible, in monumental buildings its natural application. The still existing limitations are related to several factors. In fact, the application of these procedures in the field of historic and monumental buildings, although almost systematized under the theoretical

point of view, finds difficulties associated with: (i) the selection and proper design of the monitoring network (with regard to both the choice of the optimal sensor layout on the structure and the design of the sensor system itself); (ii) the operational difficulties associated with the management of the large amount of data coming from a long-term dynamic monitoring network; (iii) the dependence of the modal properties on the environmental parameters; (iv) the evaluation of the effects of a potential structural damage on the modal properties.

### 2.1. Network architecture

Before reporting on the chosen architecture, it is worth noting that the design of the proposed wireless monitoring system takes into account several peculiar aspects. First, the monitoring system is composed by different kinds of nodes, with different kinds of sensors: accelerometers, strain gauges, displacement transducers, environmental monitoring devices (temperature, humidity, wind). Each sensor (and then each node) has its special requirements, in terms of sampling frequency, data storage and radio data rate. Another important aspect is represented by the sample synchronization. This phase is critical when dealing with structural data analysis, since every bunch of data must be correlated with the others. Therefore, a robust network synchronization algorithm is needed. Another aspect taken into account is represented by the packaging of the accelerometers that must be mechanically suitable for the detection of very small vibrations at low frequencies. This implies direct adherence between the sensor and the box itself. Moreover, from the packaging point of view, since the system is installed over historical buildings often visited by tourists, it is important to ensure compliance with local regulations, protection against tampering and respect for aesthetics. Finally, another constraint is represented by the remote control of the entire wireless monitoring system, needed in order to avoid frequent access to the structure

To meet all the above requirements, a custom hardware, firmware and software solution was designed.

The network architecture showed in Figure 1 guarantees the sensor heterogeneity constraint as well as the remote control of the entire monitoring system. Indeed, the central element is the message queue telemetry transport (MQTT) broker, which forwards all messages between the sensors and the rightful receivers. Each sensor is connected to a gateway that publishes a message to the broker including a topic (i.e., acceleration, temperature and humidity) in the message.

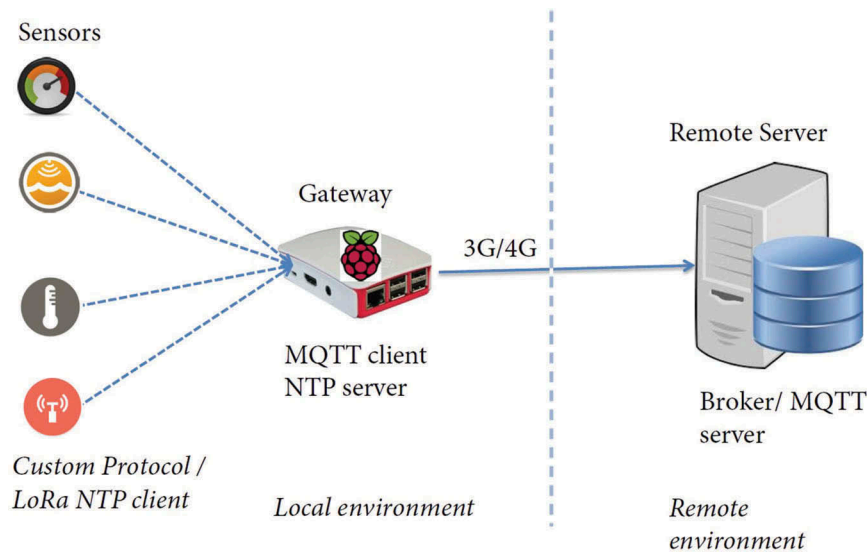


**Figure 1.** Monitoring system network scheme.

The gateway is the node that allows the integration of the different kinds of sensor technologies. In particular, the gateway allows a two-way communication: from sensors to the monitoring center, for the transmission of collected data, and from the monitoring center to the nodes, allowing the remote parameter configuration via a simple and convenient Web interface. [Figure 2](#), as an example, reports a view of the gateway as installed on the historic tower here analysed.

Each application/service that wants to receive messages subscribes to a topic, and the broker delivers all messages with the matching topic to the applicant. This architecture allows scalable solutions without



**Figure 2.** View of the gateway (installed on the tower case study).

dependencies between the data producers and the data consumers, and it is ideal for the emerging IoT/machine-to-machine (M2M) world, where bandwidth and power consumption are of paramount importance ([Barsocchi et al. 2018](#)).

Moreover, the gateway, by connecting directly to the broker with connection failover and message-buffering mechanisms, prevents data loss when connectivity issues arise on the Internet Protocol network ([Barsocchi et al. 2014](#)). The sensing information received through the messaging service is stored in two different databases. In particular, a MySQL database stores part of the wireless sensor (WS) information, while a MongoDB database stores the remaining part. The MySQL database is used to store sensor identification, the type of data acquired, and the medium access control address of the sensor nodes. Instead, the MongoDB non-relational is used to store all the sensing information gathered from the WS nodes.

The synchronization constraint is guaranteed by using the internal clock with the Network Time Protocol (NTP). Each node is endowed with an NTP client, and, just before the acquisition, each node sends a timing request to the local NTP server.

## 2.2. Sensor nodes

Considering the expected functionalities and the need to strongly adapt the system to the application context, the realization of an “ad hoc” node was considered the optimal solution. The designed node platform has a modular and easily expandable architecture ([Figure 3](#)). Every node is composed by a combination of:

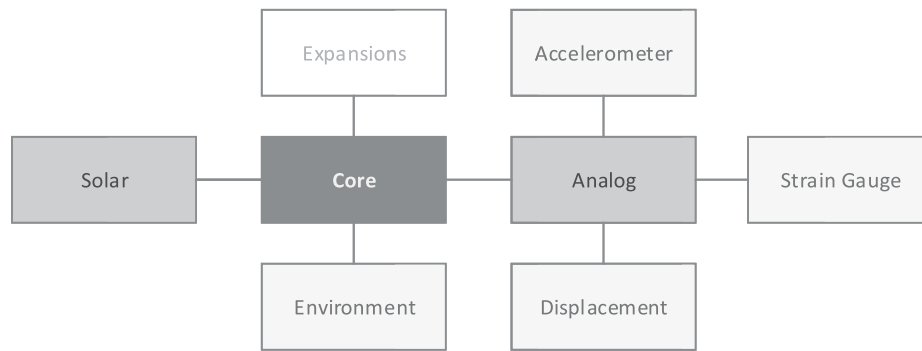


Figure 3. Node modules block diagram.

- *Core board*, delegated to the collection, processing and sending of data (Figure 4a). The Core board provides computation and communication functionalities to the system, coordinating the different parts of the node. The diagram reported in Figure 5 represents the basic components of the board. The main component is the microcontroller, a ST Microelectronics STM32F4. Local data is stored on FRAM memory when dealing with high throughput sensors (such as accelerometers). Unlike Flash and Micro SD, FRAM provides faster read/write operations and lower power consumption (but lower capacity). The Micro SD, instead, is used to maintain limited access to read/write data, such as node status and configuration, local logger (saved into easily readable TXT files), and so on. The user interface (and specifically the display,  $128 \times 48$  OLED) is useful when testing or installing the system: it provides handy information such as node identifier, hardware/firmware version, acquisition status, data link activity, battery power etc. (Figure 6). The programming and debug interface, available both on Micro USB connector and SWD (IDC), is rich and easy to use; the board is completed by an expansion connector Arduino-compatible, used when additional boards or components are needed.
- *Solar board*, used when direct supply is not available and battery-operated supply with solar panel charging is required (Figure 4b);
- *Analog board*, needed to condition and convert acceleration, displacement and strain gauge signals (Figure 4c).

With regard to the transducers, the *Accelerometer* node (Figure 7) consists of a custom sensor board, based on a mono-axial MEMS transducer with differential analog output, developed by Safran Colibrys SA. This sensor is characterised by very high sensitivity ( $1.35 \text{ V/g}$ ), large and flat frequency response (from DC to 7 kHz) and ultra-low noise output ( $7 \mu\text{g}/\sqrt{\text{Hz}}$ ). The full-scale selected is  $\pm 2\text{g}$  (typical), because we deal with very low signal amplitudes. Besides the accelerometer transducer, this module includes pre-filtering and buffering stages. The first is used to remove unwanted frequency components from the signal, thereby reducing the overall noise. The second allows the use of longer cables between the sensor and the acquisition box, without significant signal loss and/or corruption.

In the case of the *Strain Gauge* node, a commercial Pi-shape transducer with differential output has been selected: specifically, the TML PI-2 with gauge length of 300mm. This device is a combination of strain gauges and an arch-shaped spring plate, the former attached to

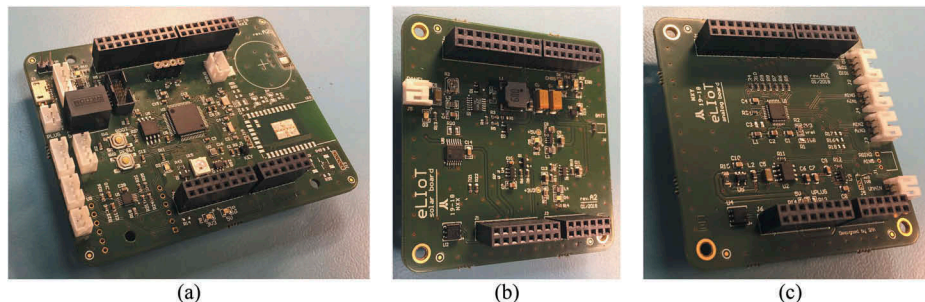


Figure 4. Core (a), Solar (b) and Analog (c) boards.

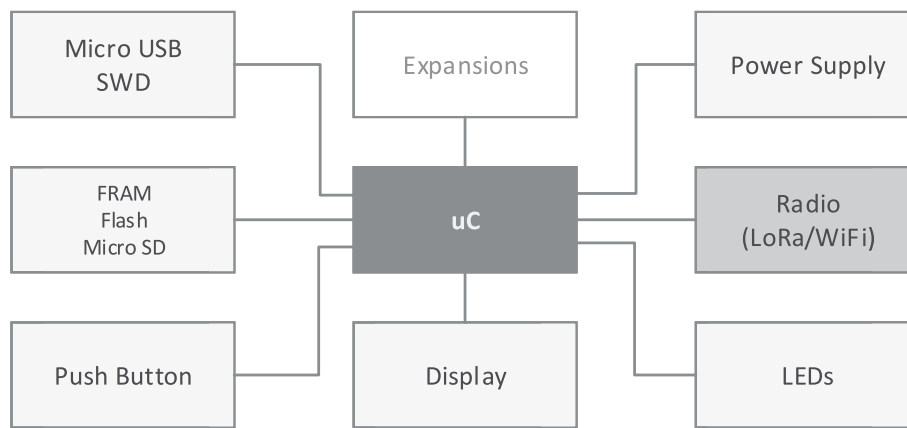


Figure 5. Block diagram of the core module.

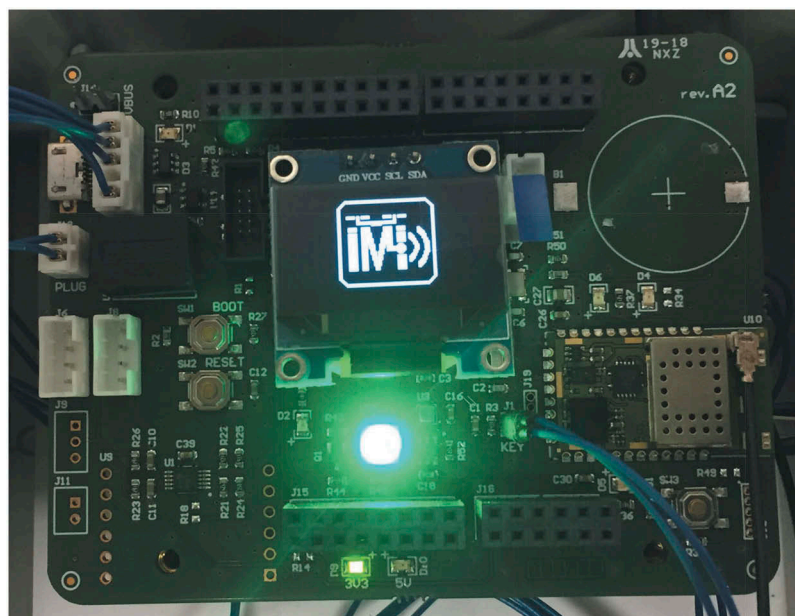


Figure 6. Node display, LEDs and push buttons.

the latter. The transducer is connected to the node, and its signal is adapted and converted by the *Analog* board. The *Displacement* node is similar to the previous one, but in this case, a Gefran PZ67 auto-aligning potentiometric transducer with single-ended output is used, whose signal was fed to the *Analog* board, for signal conditioning and conversion. Finally, the *Temperature/Humidity* node makes use of a commercial sensor made by Davis, equipped with a Sensirion SHT31 precision transducer with digital output. The reading is then directly processed by the *Core* board.

### 2.3. Packaging and layout

Starting from the described modular architecture, different types of nodes were assembled: accelerometer,

strain gauge, displacement, temperature/humidity (indoor) and complete weather station (outdoor). As mentioned, display was provided on-board to allow ease reading of the operating parameters. A multi-colour status LED is also provided to allow malfunction identifying even at long distance. To this end, IP67 boxes with semi-transparent cover were chosen, compatible with outdoor installation and protected against dust and atmospheric agents (rain, wind). Moreover, the selected panel connectors are also IP67 certified and allow easy plug and/or replacement.

The accelerometric transducers were assembled keeping the board as close as possible to the box, to avoid the introduction of extraneous signals produced by the mechanical coupling between the transducer and the box itself. There is a single connector on the panel,

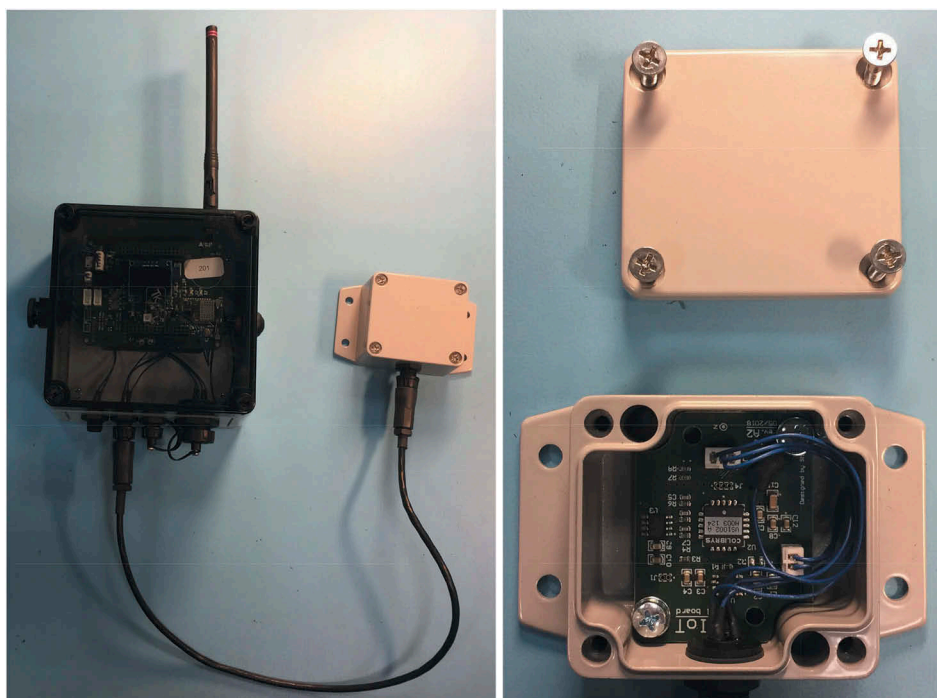


**Figure 7.** The accelerometer node with custom sensor board and box.

needed for power supply and connection of the transducer signal to the acquisition node.

#### 2.4. Test and validation

The operation of the new sensors was verified through a set of laboratory tests and the data acquisition and pre-processing routines were improved in order to ensure the best possible performance over. In particular, a comparison was performed between the performances of the developed system and those of a commercial reference one (a monoaxial piezoelectric accelerometer PCB 393C).

The measurement was carried out using an oscillating structure with a known resonance frequency. A wooden-framed structure was built (Figure 8), consisting of two 1 m high columns with rectangular cross section of (10 mm × 98 mm), spaced about 350 mm and connected to an upper wooden beam with rectangular cross section of (34 mm × 94 mm). All connections are ensured through steel angle brackets and bolts; this setup prevents any relative rotation of the elements composing the wooden structure, whose fundamental frequency can be tuned by simply adding or removing sandbags from the upper beam. Without additional masses on the top of the structure, the fundamental frequency of the system is equal to 3.70 Hz, as also confirmed via finite-element simulation (Barsocchi et al. 2018).

Comparisons between the developed sensor and the reference accelerometer were performed in both the frequency and the time domain, on the values of the fundamental frequency measured by the two devices and on the shape and trend of the experimental signals recorded. The devices were tested on the structure under ambient vibration and then assigning a horizontal displacement to the upper beam and measuring the resulting oscillations of the system; each experiment was repeated four times. Figure 9a shows the very good correspondence between the signals recorded by the two devices, while in Figure 9b the performances of the accelerometers are compared in terms of frequency content.

### 3. The case study

The case study selected to test the efficiency of the designed Wireless Sensor Networks is the Matilde Tower in Livorno (Italy). This is a historic masonry tower built in the Livorno harbour, which belongs to an old architectural site called “*Fortezza Vecchia*” (Old Fortress). This structural typology is iconic and widespread all over the Mediterranean area and generally exhibits high vulnerabilities with respect to the horizontal loads (Acito et al. 2014; Bartoli et al. 2019; Bartoli, Betti, and Monchetti 2017; Ivorra, Pallarés, and Adam 2009).

The Matilde Tower (Figure 10) was built in the XIII century as a stand-alone structure and was modified through the time. Nowadays it appears as a massive



(a)



(b)

**Figure 8.** The wooden oscillating structure used for the validation (a) and the developed accelerometer (b).

tower bounded by the fortress walls and by several small buildings. The structure has a circular section with an external diameter of about 12 m and a total height of about 29 m. The walls width is 2.5 m and a helicoidal stair is embedded in the walls to reach the different levels. The slabs are constituted by masonry vaults and concrete, giving a rigid-plane behaviour to the structure. The masonry vaults at Level 0 (Figure 11) were retrofitted in the past with four tie rods.

The tower is surrounded by the walls of the fortress and other minor buildings reaching different heights. The South-West corner is bounded by the original block of the fortress called “*Quadratura dei Pisani*”,

and the East side is confined by the ruins of the Cosimo dei Medici palace. The entire architectural complex suffered several damages, due to foundations settlements, environmental erosion phenomena and bomb attacks occurred during the World War II.

The presented case study can be considered an interesting application since it is subjected to a wide spectrum of dynamic excitations caused by traffic, remarkable wind speeds, and the harmonic forced vibrations generated by the engines of the ferry boats docked in the harbour.

### 3.1. Preliminary dynamic tests

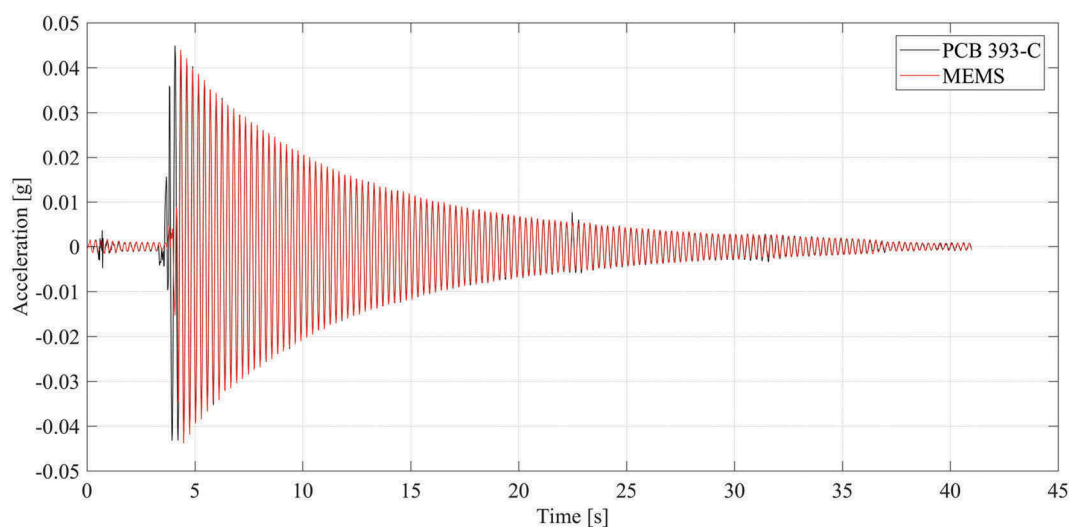
Preliminary dynamic tests were performed on the 23th of January, 2017 by the DICEA-UNIFI Lab, using 12 high sensitivity piezoelectric accelerometers (PCB 393-C with a range of 2.5 g, sensitivity of 1 V/g and PCB 393-B31 with a range of 0.5 g, sensitivity of 10 V/g), in order to characterize the dynamic behaviour of the tower. The prior knowledge of the dynamic behaviour is in fact a basic datum for the design of a suitable long-term monitoring system, especially for the CHS. For this reason, the preliminary dynamic campaign was performed using a refined grid of sensors in order to identify the dynamic behaviour of the tower and design the sensor setup of the long-term monitoring system.

For the sake of brevity, herein the only results of the preliminary dynamic campaign are reported. Specific details of the experimental layout are reported in Zini et al. (2018). The signals were recorded with a sampling frequency of 400 Hz, filtered in the frequency band 0.3–13 Hz with two fourth order low-pass/high-pass Butterworth filters and down-sampled to 30 Hz.

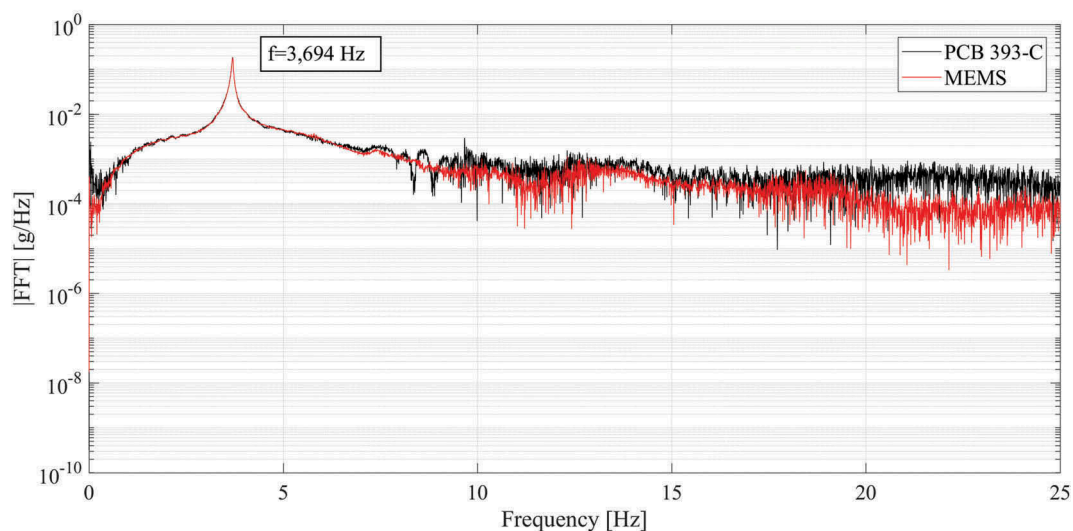
From the analysis in the frequency domain via the Frequency Domain Decomposition (FDD) technique, the presence of harmonic responses was observed by the local increase in the rank of the Power Spectral Density (PSD) matrix in proximity of the narrow band peaks (Figure 12). The results of the dynamic identification are summarized in Table 1. They were obtained by comparing two techniques: the FDD in frequency domain and the data driven Stochastic Subspace Identification (SSI-data) in time domain. The results obtained with the two techniques show a good agreement between them both in terms of frequency and mode shapes (reported in Figure 13).

### 3.2. Finite-element modelling and model updating

A finite element (FE) model of the Matilde Tower was built making use of the NOSA-ITACA code (Girardi, Padovani, and Pellegrini 2015). The tower model



(a)



(b)

**Figure 9.** System validation: (a) comparison between the horizontal accelerations recorded by the developed sensor (MEMS) and the reference accelerometer (PCB); (b) fast fourier transform (FFT) of the signals recorded by the developed sensor (MEMS) and the reference accelerometer (PCB).

consists of 44,092 isoparametric 8-node brick elements (element 8 of NOSA-ITACA library), for a total number of 160,299 degrees of freedom (Figure 14). The nodes of the model were fixed at the base, while the constraints given by the curtain walls of the Old Fortress were simulated via lateral springs.

Considering the lack of information about the composition and the mechanical properties of the masonry constituting the tower walls, a homogeneous material was considered in the model: in particular, once fixed the mass density to  $2,000 \text{ kg/m}^3$ , the Young's modulus of masonry and the stiffness of the lateral springs were

tuned in order to fit the experimental values of the natural frequencies by using the model updating algorithm proposed in Girardi et al. (2019). Table 2 shows the eigenfrequencies of the finite-element model obtained for a Young's modulus of 2,500 MPa and a stiffness of the lateral springs of  $5.1 \cdot 10^9 \text{ N/m}$ . A comparison with the experimental values is also reported in Table 2: the finite element model fits very well the first two frequencies, corresponding to bending modes, but exhibits a stiffer behaviour on the highest frequency. The numerical results highlight also an intermediate frequency at 6.2 Hz, corresponding to an axial-



**Figure 10.** View of the Matilde Tower with the surrounding structures.

torsional mode, which has not been clearly identified in the preliminary experimental tests. The first, second and fourth mode shape of the finite element model are also illustrated in [Figure 15](#).

#### 4. Automatic modal parameters extraction

The automated procedure proposed here for the extraction of the modal parameters is constituted by the following steps: (i) signal acquisition and processing, (ii) input selection, (iii) system identification through the covariance driven Stochastic Subspace Identification (Van Overschee and De Moor 1996) (SSI-cov), (iv) clustering phase (Cheynet, Jakobsen, and Snæbjörnsson 2016; Magalhães, Cunha, and Caetano 2009; Reynders, Houbrechts, and De Roeck 2012; Ubertini, Gentile, and Materazzi 2013) and (v) statistical processing of the obtained data. All these steps are needed for the dynamic characterization of the investigated structure and the vibration sources, allowing a clear identification of the modal parameters (Ceravolo et al. 2017).

The procedure was implemented in a MATLAB routine which automatically processes the data acquired by the monitoring system ([Figure 16](#)) with a sampling frequency of 50 Hz. The raw data are then filtered in the frequency band 0.3–10 Hz by applying successively two fourth-order low-pass/high-pass Butterworth filters and down sampled to a frequency of 25 Hz. The obtained modal parameters are tracked through the monitored period and correlated with the environmental effects.

The whole algorithm implemented for the modal parameters extraction (illustrated in [Figure 17](#)) was previously calibrated over a week of acquisition, in order to define the energy level threshold for the selection of the inputs.

##### 4.1. Calibration of the algorithm

The calibration of the algorithm, with respect to its three main phases (*Input Selection, Modal Identification and Modal tracking*), was performed over a suitable starting period.

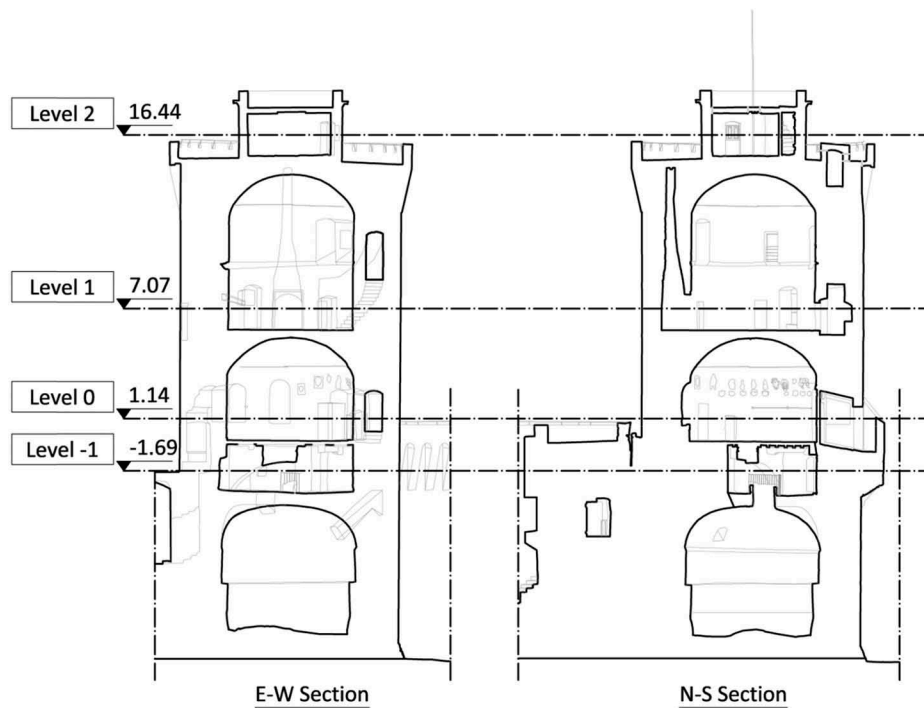


Figure 11. Longitudinal and transversal section of the Matilde Tower.

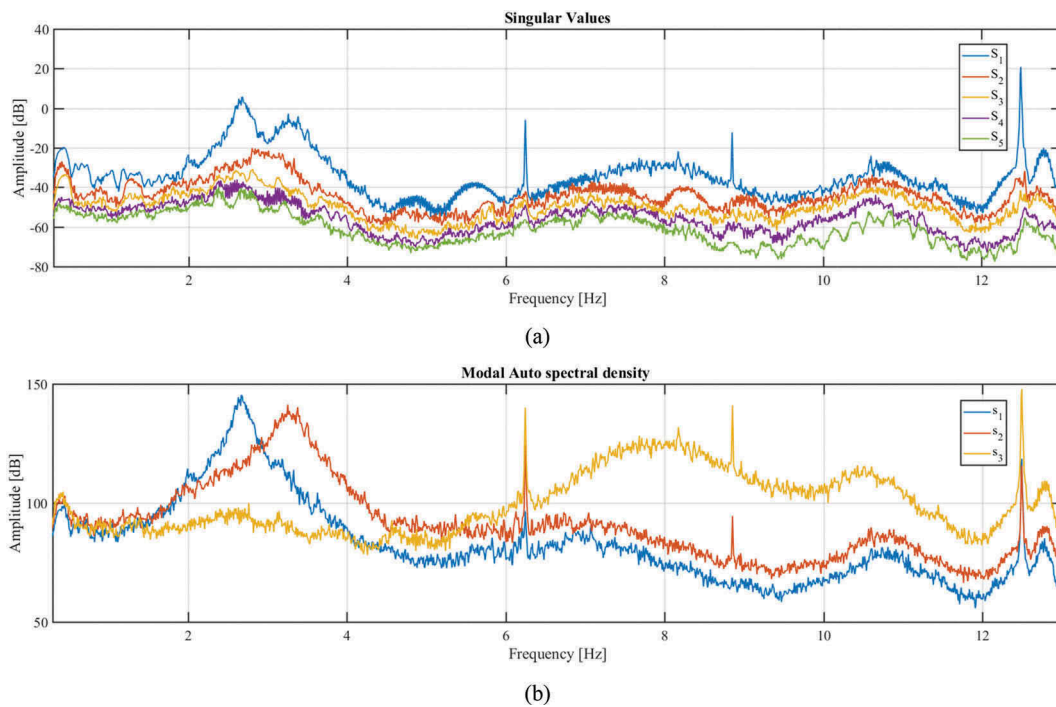


Figure 12. Frequency analysis of the preliminary tests: (a) The first five singular values of the power spectral density matrix (PSD); (b) Auto-spectral density estimation of the first three modes via modal filtering.

For the input selection, the calibration phase gives the reference values of the Root Mean Square (RMS) and the Signal-to-Noise-Ratio (SNR) that allow the identification of a minimum number of modes  $N$ . The calibration phase also contributes to a suitable

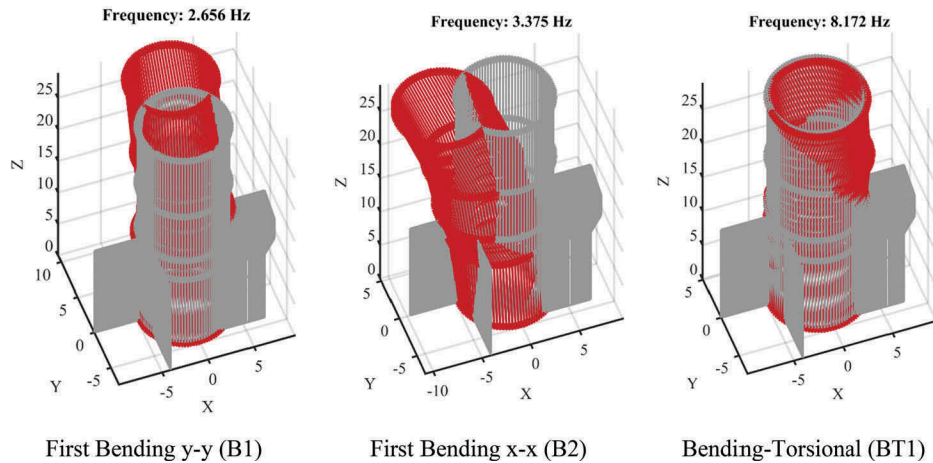
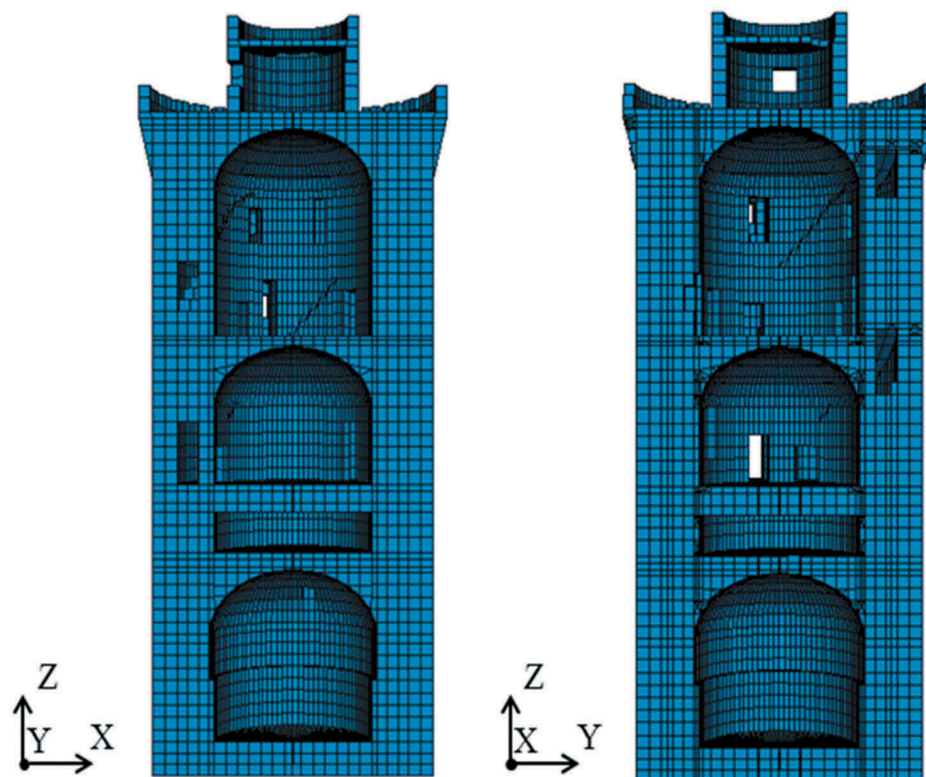
definition of the optimum number of rows in the Henkel matrix and of the model order range of variation, by means of a sensitivity analysis (Rainieri and Fabbrocino 2014; Reynders, Pintelon, and De Roeck 2008).

**Table 1.** Results of the preliminary identification test.

Identified mode	Frequency (Hz)		Damping ratio (%)		MAC
	FDD	SSI-data	FDD	SSI-data	
Mode 1 (translational y-y)	2.656	2.685	-	3.20	0.998
Mode 2 (translational x-x)	3.375	3.367	-	3.20	0.990
Mode 3 (bending-torsional)	8.172	8.202	-	2.70	0.973

To validate the obtained results, the complexity of the mode shapes was investigated using the Mean Phase Deviation (MPD) and the Modal Phase Collinearity (MPC) (Reynders, Houbrechts, and De Roeck 2012).

These two indicators exhibit values between 0 and 1 and can be used to discriminate the physical from the spurious modes in a proportionally damped system. MPC values equal to one indicate real modes. The MPD indicator measures the angle of the best straight line fitting a mode shape in the complex plane (Reynders, Houbrechts, and De Roeck 2012) (it is measured in degree); values equal to zero are attributable to real modes. In this paper the MPD indicator is the reciprocal of the classic definition, thus giving values equal to one for

**Figure 13.** The first three modes identified with the FDD. The y axis is approximately the N-S direction and the x axis is the E-W.**Figure 14.** Finite-element model of the Matilde Tower. The y axis is approximately in the N-S direction and the x axis is in the E-W direction.

**Table 2.** Matilde Tower: experimental ( $f_{\text{exp}}$ ) and numerical ( $f_{\text{num}}$ ) frequencies and relative errors ( $\Delta f$ ).

$f_{\text{exp}}[\text{Hz}]$	$f_{\text{num}}[\text{Hz}]$	$\Delta f$ [%]
2.685	2.67	-0.56
3.367	3.34	-0.81
-	6.26	-
8.202	9.71	18.39

the real modes and to zero for the complex modes. Anyway, complex mode shapes can arise from both non-linearity in the structural behaviour and noise in the measurements. Hence, the thresholds on MPC and MPD values for defining the real modes was set in a statistical way, through the results obtained over the calibration period. The calibration phase allows also defining the MAC values for the Modal Tracking (MT) of the identified modal parameters.

As shown in Reynders, Pintelon, and De Roeck (2008), the variance in the estimation of the Modal Parameters (MP) is strictly connected to the operative conditions (coloured noise, non-stationarity, SNR ratio). The aim of the calibration phase is to reduce the uncertainties that affect the identification process and to check the quality of the input data, in order to increase the accuracy of the identified modal parameters (Marwitz and Zabel 2018). All these operations are needed because the frequency variations potentially induced by damage are very low and can be buried by the environmental effects; hence, a prior reduction of the errors and noise is very important for the correct application of the SHM algorithm.

For the investigated structure, the main source of excitation is the wind; for this reason, two periods of calibration were chosen (Figure 18, Figure 19). The first (#P1) was the week with the highest values of recorded wind speed (3/12/2018-10/12/2018), and the second (#P2) was the week with the lowest wind speeds (15/02/2019-22/02/2019). Thus, suitable thresholds for the input selection, the modal identification and the modal tracking are defined considering both the excitation levels.

#### 4.2. Input selection

The input selection allows choosing the records with the highest quantity of modal information. Indeed, the level of excitation described, for each sensor, by the power of the signals in terms of Root Mean Square (RMS) is one of the key reference parameters. To check the quality of the input signals, the fourth order statistical moment (Kurtosis) of each time history was also calculated.

The Kurtosis gives some indications about the Probability Density Function (PDF) of the time

histories. In particular, values equal to 3 indicate that the PDF is Gaussian, higher values mean that the distribution exhibits higher tails. Values lower than 3 mean that some periodic wave is inside the signals (e.g. a sine wave has a Kurtosis equal to 1.5). Hence, the Kurtosis values were used to check the hypothesis that the recorded signals come from a Gaussian white-noise process.

Usually, in the OMA testing the signal quality assessment is performed by checking the SNR ratio. For instance the American standards ANSI S2.47 (1990) recommend a minimum level of 5 dB and they propose some corrections in the range between 5–10 dB. Anyway, some Authors (Brincker and Ventura 2015) suggest a minimum level of 30–40 dB for the OMA identification of large civil structures.

Considering the main dynamic input of the Matilde Tower, i.e. the wind (Figure 20), a criterion for the input selection was defined through the analysis of the calibration phase results. The analysis of the Kurtosis allows detecting abrupt changes in the signals like spikes and dropouts due to the system malfunctioning (Figure 21). To avoid these phenomena, an outlier analysis was performed and all the values outside 1.5 times the interquartile range were excluded.

For the sake of simplicity, and to fix a unique value for all the inputs, the thresholds on the RMS, SNR and Kurtosis were finally defined as the mean values of those coming from all the accelerometers (Table 3). Conservatively, for the SNR and the RMS values the threshold coincides with the lower bound of the interquartile range (Figure 22). Instead, the Kurtosis threshold was assumed as 1.5 times the upper bound of the interquartile range, in order to avoid loss of data in the case of large distribution tails generated by strong wind effects (Table 4).

#### 4.3. Automated modal identification

The Stochastic Subspace Identification (SSI) (Van Overschee and De Moor 1996) is a well-established parametric technique in the time domain used for the Operational Modal Analysis (OMA). The structure, subjected to unknown input, is modelled in the time domain as a discrete linear time-invariant system, whose dynamic behaviour is governed by the following state-space model (Ljung 1987):

$$\begin{aligned} \mathbf{x}_{k+1} &= \mathbf{A}\mathbf{x}_k + \mathbf{w}_k \\ \mathbf{y}_k &= \mathbf{C}\mathbf{x}_k + \mathbf{v}_k \end{aligned} \quad (1)$$

where  $\mathbf{x}_k \in \mathcal{R}^N$  is the state space vector describing the system in the stochastic space,  $N$  is the model order, and  $\mathbf{y}_k \in \mathcal{R}^l$  is the vector of observations at the  $k$ -th time

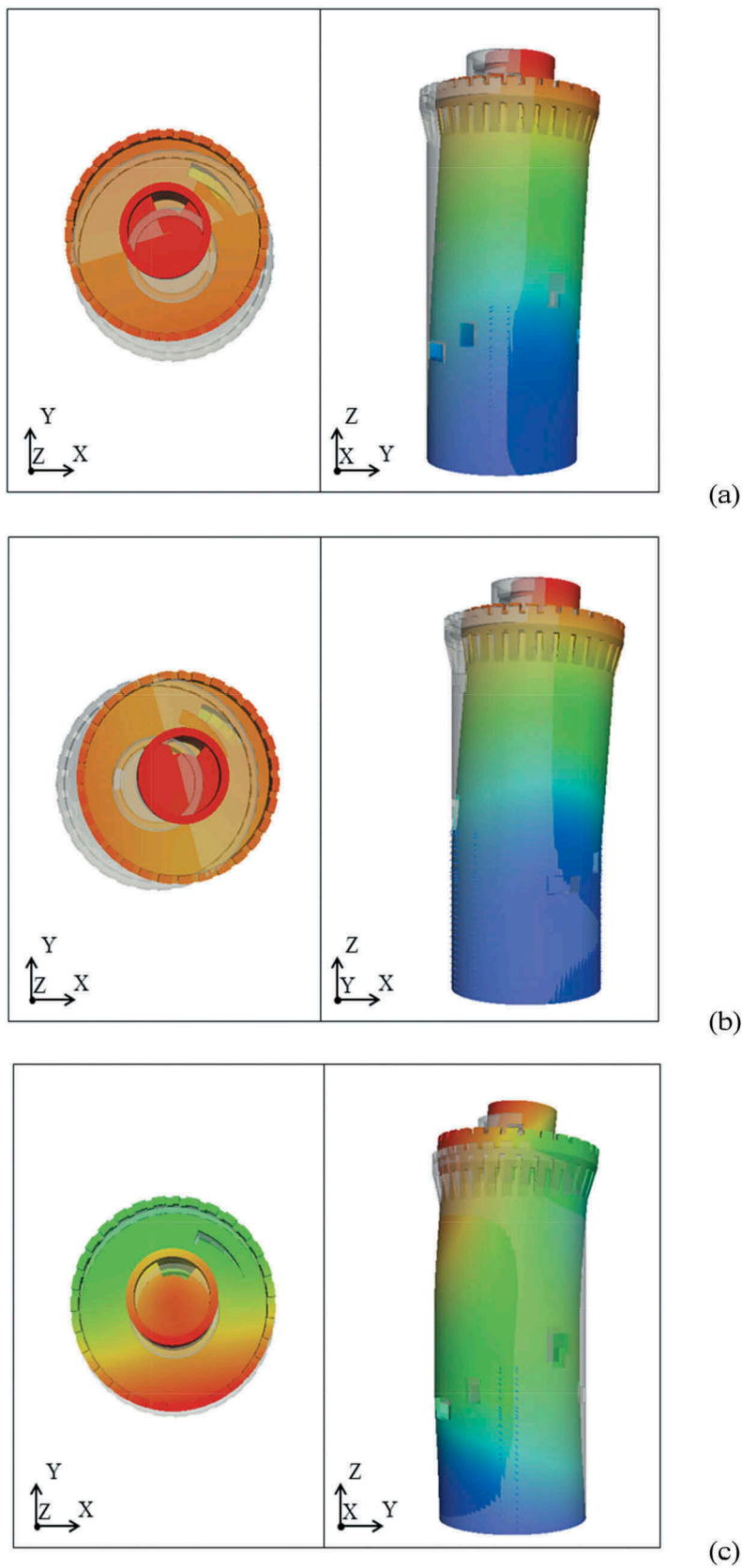


**Figure 15.** Finite element model: (a) first mode shape; (b) second mode shape and (c) fourth mode shape. The y axis is approximately in the N-S direction and the x axis is in the E-W direction.

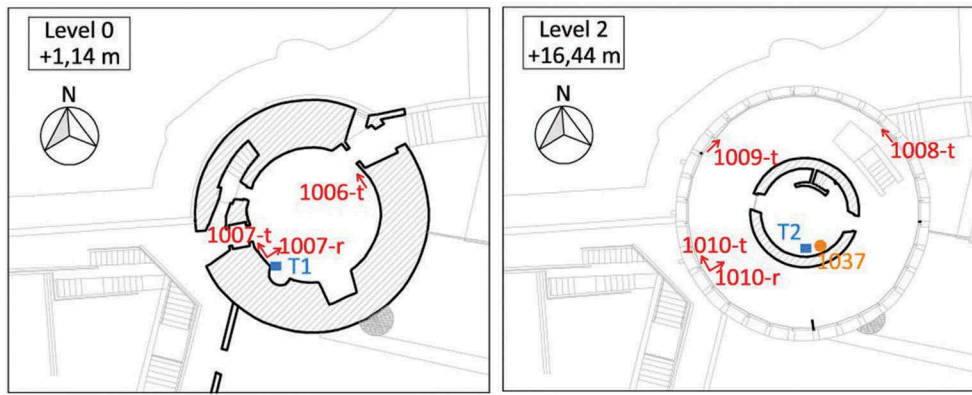


Figure 16. Layout of the sensors in the MOSCARDO monitoring system. The red arrows are the accelerometers, the blue squares are the meteorological stations and the anemometer is in yellow.

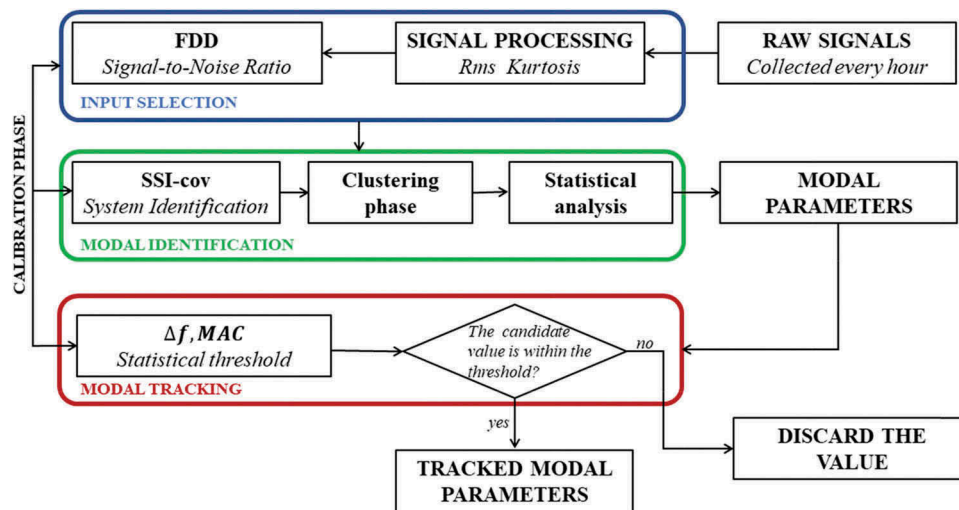


Figure 17. Flowchart of the automated modal identification algorithm.

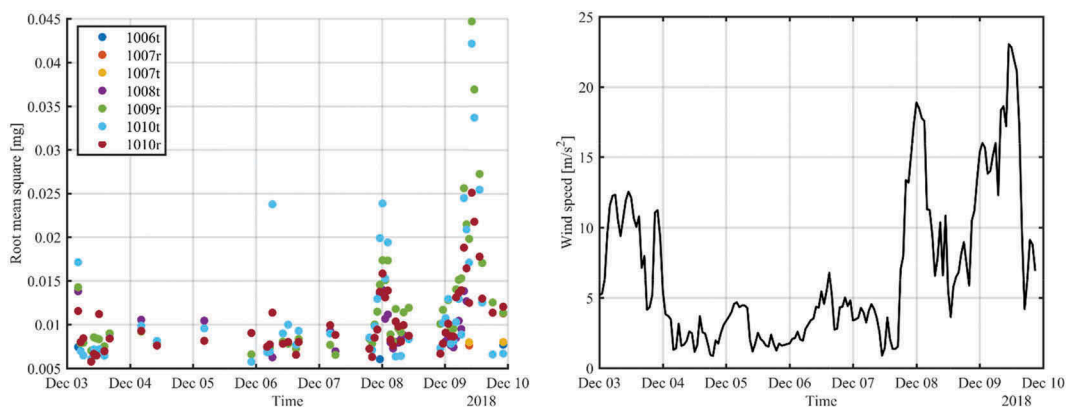


Figure 18. Root mean square values and wind speed over the first calibration period (#P1 3/12/2018-10/12/2018).

step. The vectors  $\mathbf{w}_k \in \mathcal{R}^N$  and  $\mathbf{v}_k \in \mathcal{R}^l$  are two unknown zero mean white noises modelling the process noise (the unmeasured inputs can be considered part of the process noise) and the output noise, respectively. The

$N \times N$  matrix  $\mathbf{A}$  and the  $l \times N$  matrix  $\mathbf{C}$  are the system matrix and the controllability matrix, representing the evolution of the state-space configuration in the stochastic space and the representation of the sequence of

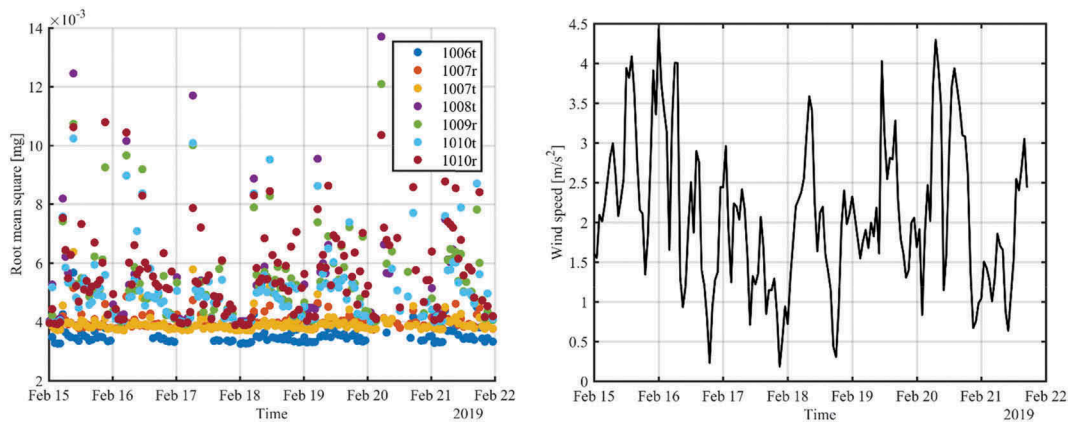


Figure 19. Root mean square values and wind speed over the second calibration period (#P2 3/12/2018-10/12/2018).

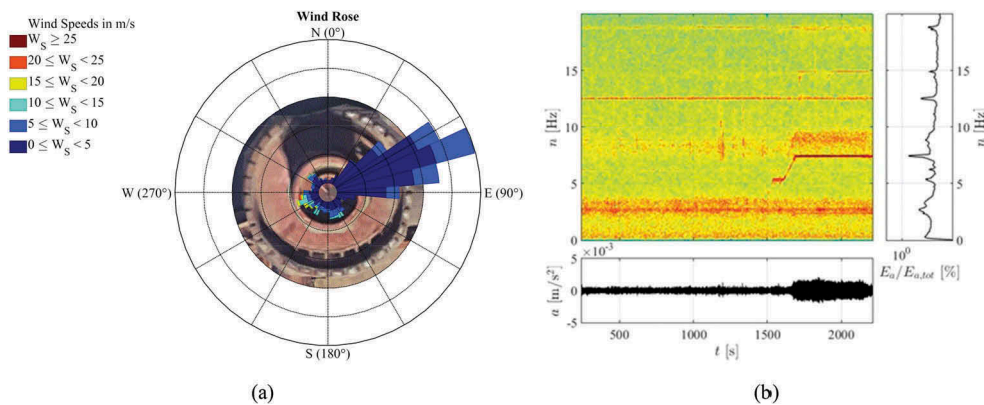


Figure 20. (a) Average wind direction; (b) the Short Fourier Transform (SFT) of the recorded signals at the last level in the preliminary dynamic campaign.

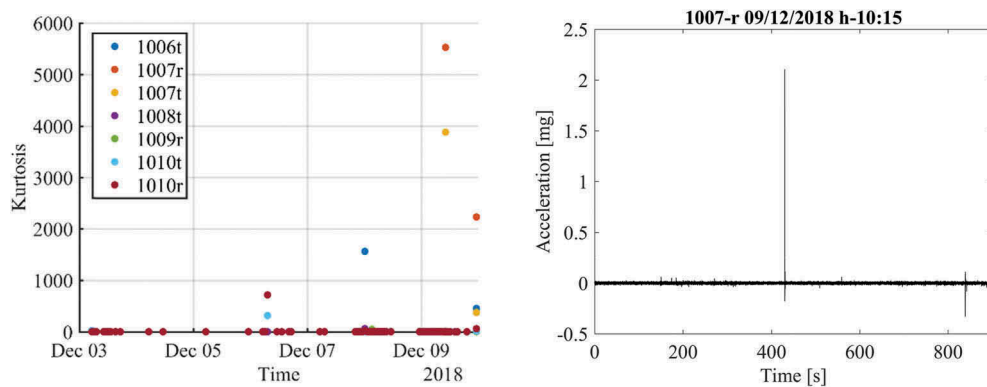


Figure 21. High values of the Kurtosis usually imply spikes or dropouts in the signals.

observation in the space of the measured DOFs, respectively. Thus, it is possible to identify the system modal characteristics from the eigenvalues decomposition of the system matrix (Peeters and De Roeck 2001).

The algorithm here used for the modal identification is the so-called Principal Components algorithm based on the decomposition of the Toeplitz block matrix,

estimated from the covariance matrices of the signals. The model order  $N$  is linked to the number of system modes (a system with a model order  $N$  has  $N/2$  modes). The choice of the optimal model order is not straightforward, due to the noise effects. Then, a range of model order variation should be decided in advance and the modal parameters can be selected by visual

**Table 3.** Statistical properties of the input values obtained on the two-calibration periods (#P1, #P2). The RMS and the Kurtosis are the mean values of all the instruments.

Calibration phase	SNR [dB]		RMS [mg]		Kurtosis	
	median	Dev. Std.	median	Dev. Std.	median	Dev. Std.
#P1	46.26	10.63	0.0099	0.0067	5.14	240.87
#P2	43.45	12.94	0.0047	0.0014	3.05	72.29

inspection of the stabilization diagram, as repeated poles at every model order. Usually, the minimum model order is fixed in twice the minimum number of expected modes, while the maximum is much higher. This operation, called over modelling, introduces some spurious modes that can bring to misleading values.

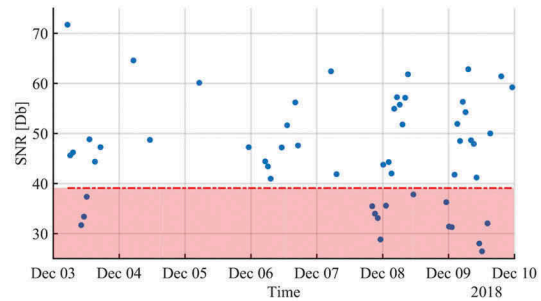
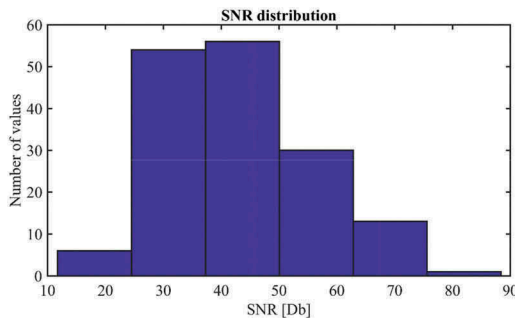
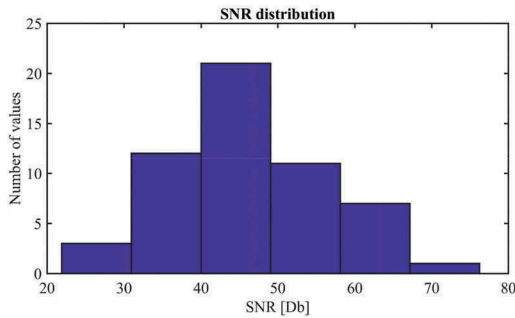
An optimum value of the number of rows in the Henkel matrix, representing the memory of the process, should be defined in advance by means of a sensitivity analysis (Cabboi et al. 2017; Rainieri and Fabbrocino 2014). The automated interpretation of the stabilization diagram was performed with a single linkage hierarchical clustering algorithm (Magalhães, Cunha, and Caetano 2012) and the candidate modes were subsequently validated with two single mode validation criteria: the Modal Phase Collinearity (MPC) and the Mean Phase Deviation (MPD) (Shih et al. 1988). The values of the MPC and MPD thresholds were selected as the mean of the values obtained through the calibration phase (Table 5). It is

worth noting that complex modes can arise from different phenomena (Imregun and Ewins 1995). On the one hand the complexity deals with measurements errors and identification issue, on the other hand the complexity can arise from the non-linear behaviour of the structure and from aerodynamics effects. Hence, it is crucial to define conservative thresholds from data collected in the calibration period, avoiding the loss of information dealing with the structural dynamics.

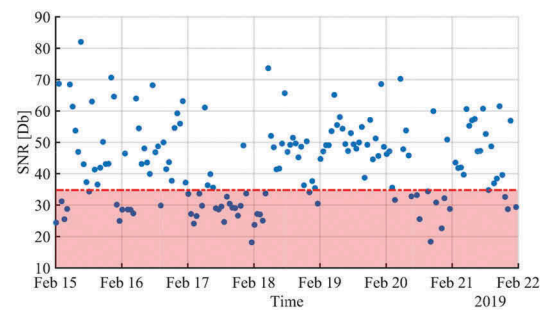
The minimum number of elements in each cluster to identify physical modes was selected equal to one third of the maximum number of poles found along a frequency alignment during the analysis of the calibration signals. Each mode is correspondingly represented as the mean of the cluster in terms of frequency, damping ratio and mode shape (Figure 23).

#### 4.4. Modal tracking of the modal parameters

Modal Tracking is a widely applied technique to collect, during the monitoring period, the identified modal properties which represent the same mode. Despite its popularity, to the authors knowledge not so many papers are available in literature dealing with this procedure. Verboven et al. (2002) introduced an algorithm for tracking the modal properties of a slat track, based on the distance between the mode residue matrices. When monitoring large



(a)



(b)

**Figure 22.** Distribution of the SNR on the two calibration periods: (a) #P1, (b) #P2. The red lines represent the thresholds chosen for the inputs.

**Table 4.** Input analysis thresholds for the automated identification algorithm.

	SNR [dB]	RMS [mg]	Kurtosis
#P1	39.06	0.14	8.58
#P2	34.72	0.0034	3.73
Threshold	34.72	0.0034	8.58

structures with OMA procedures, the vector of the participation factors is not available, and the mode residue matrix cannot be calculated. Hence, the common approach is defining a reference dataset of modal properties evaluated from dynamic testing campaigns performed with a refined grid of sensors (Sinou 2009; Ubertini et al. 2016). Then, some distance thresholds are used in terms of frequencies and mode shapes (Magalhães, Cunha, and Caetano 2009) to group together modal properties representing the same mode. The method works well if the modes are clearly separated and conversely it can fail for closely spaced modes that exhibit some coupling in the modal domain. For this reasons, Cabboi et al. (2017) proposed an adaptive threshold for each mode on the basis of the distances between the frequencies and the mode shapes.

In the present case, all the identified poles in the calibration periods have been grouped together by means of a hierarchical clustering procedure with a fixed limit distance: all the clustered elements are sorted within 5% in terms of frequency and 0.7 in terms of MAC index. Then all the clusters with enough numerosity are analysed, excluding those that are less recurring in the two calibration periods. Since mode shapes are usually less sensitive to the environmental changes, the statistical properties in terms of MAC indices for each cluster element are evaluated. Finally, the tolerance in terms of frequency is fixed to the 7.5% and in terms of mode shape is chosen as the higher value of the lower bound in the interquartile range for each calibration period. Once the thresholds are fixed, the MT is performed through the whole monitoring period merging the values representing the same mode.

## 5. Environmental effects

At the beginning of the first 12 months of monitoring several system disconnections occurred which involved the environmental sensors (temperature and humidity). However, considering both the outdoor and the indoor sensors, the measured environmental parameters cover the whole monitoring timespan (Figure 24). Environmental data were used regardless the positioning of the sensor; this was considered acceptable taking into account the low differences between the indoor and outdoor recorded values, and in consideration of the absence of a heating system in the tower together with the presence of several openings.

The results of the MT (Figure 25) show the evolution of the first three modal frequencies over the first 12 months of activity of the monitoring system. The number of tracked value for the first two identified modes is comparable (1535 for the first mode, 923 for the second mode), while the third one was identified only in a limited number of sessions (85). This can be attributable to the higher level of energy needed to excite that mode.

After one year of data, some preliminary observations can still be done: the first two modes clearly exhibit an increase of the frequency with the temperature (Figure 26a), while for the third mode a decrease, with a lower level of correlation, seems to be observed. The latter can be attributable to the current dataset that cannot still allow establishing the nature of the correlation. The positive correlation with temperature is well explained in literature (Gentile, Guidobaldi, and Saisi 2016) in terms of thermal expansion of the masonry blocks and the resulting increase of the stiffness. The negative correlation effect on the torsional mode is even documented. In Ubertini et al. (2017) this phenomenon is explained with the slackening of the tie elements introduced during retrofitting works. The same behaviour seems to be observed here, due to the presence of steel bars at each vaulted level.

**Table 5.** Choice of the parameters for the automatic modal data extraction. The parameters for the identification phase are chosen by means of a sensitivity analysis; for the stabilization phase and the validation phase the values are those suggested in literature (Peeters and De Roeck 2001).

Parameters of the system identification phase		
Number of rows in the Henkel matrix [s]	Minimum model order [ord <sub>min</sub> ]	Maximum model order [ord <sub>max</sub> ]
20	10	40
<b>Parameters of the stabilization phase (Soft Criteria)</b>		
Frequency distance ( $\Delta f$ )	Damping distance ( $\Delta \xi$ )	Mode shape distance ( $\Delta \Phi$ )
0.01	0.05	0.02
<b>Parameters of the stabilization phase (Hard Criteria)</b>		
The Identified modes are complex and conjugate?		Damping Interval
Yes/No		0.005–0.1
<b>Parameters of the validation phase</b>		
Modal Phase Collinearity (MPC)	Mean Phase Deviation (MPD)	Minimum number of elements for each cluster (N <sub>cl,min</sub> )
0.582	0.570	7

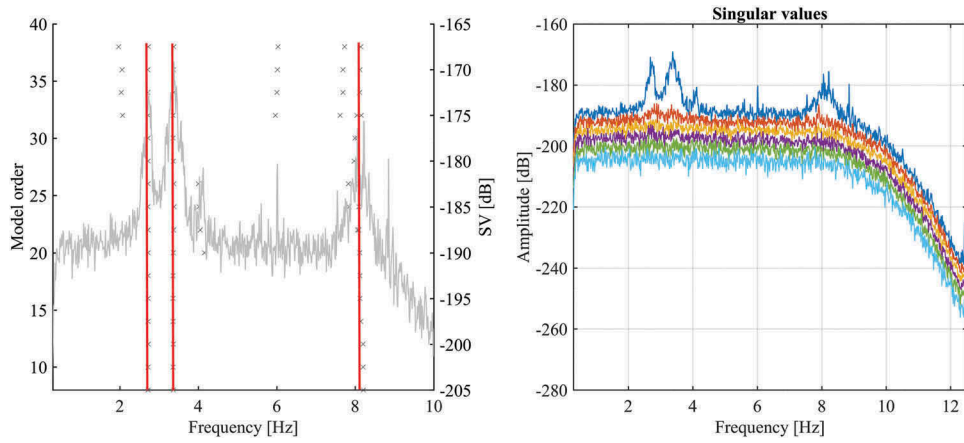


Figure 23. Stabilization diagram of the SSI-cov automated procedure and FDD (acquisition of the 12th of March at 14:15).

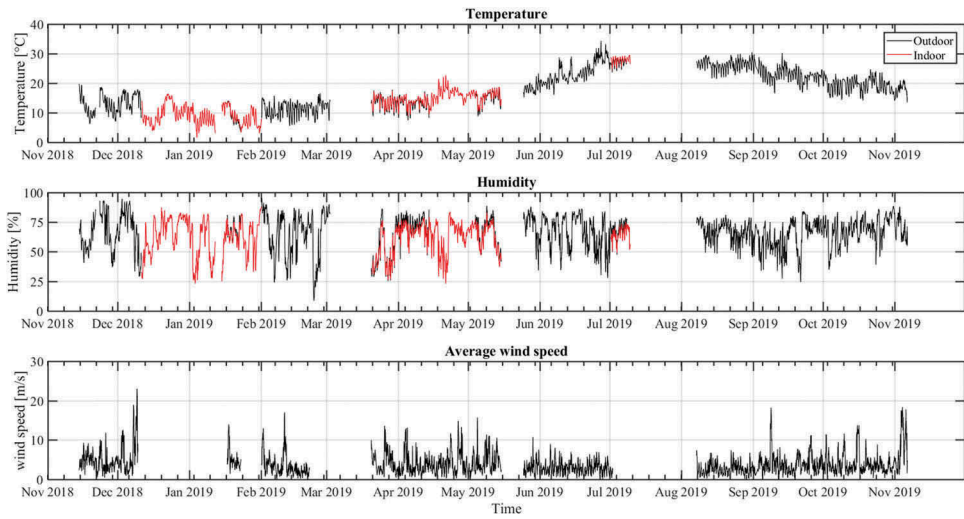


Figure 24. Variation of the considered environmental parameters over the monitored period.

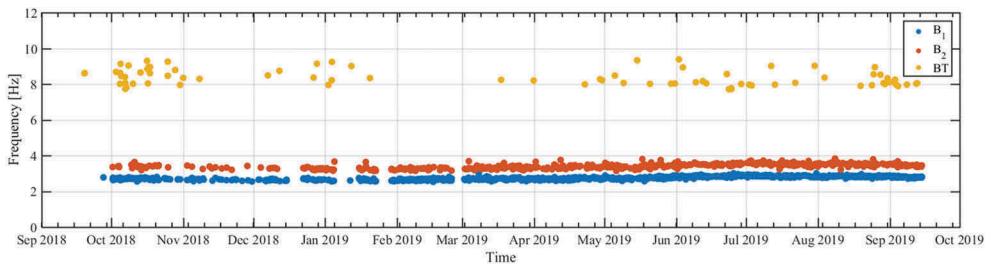
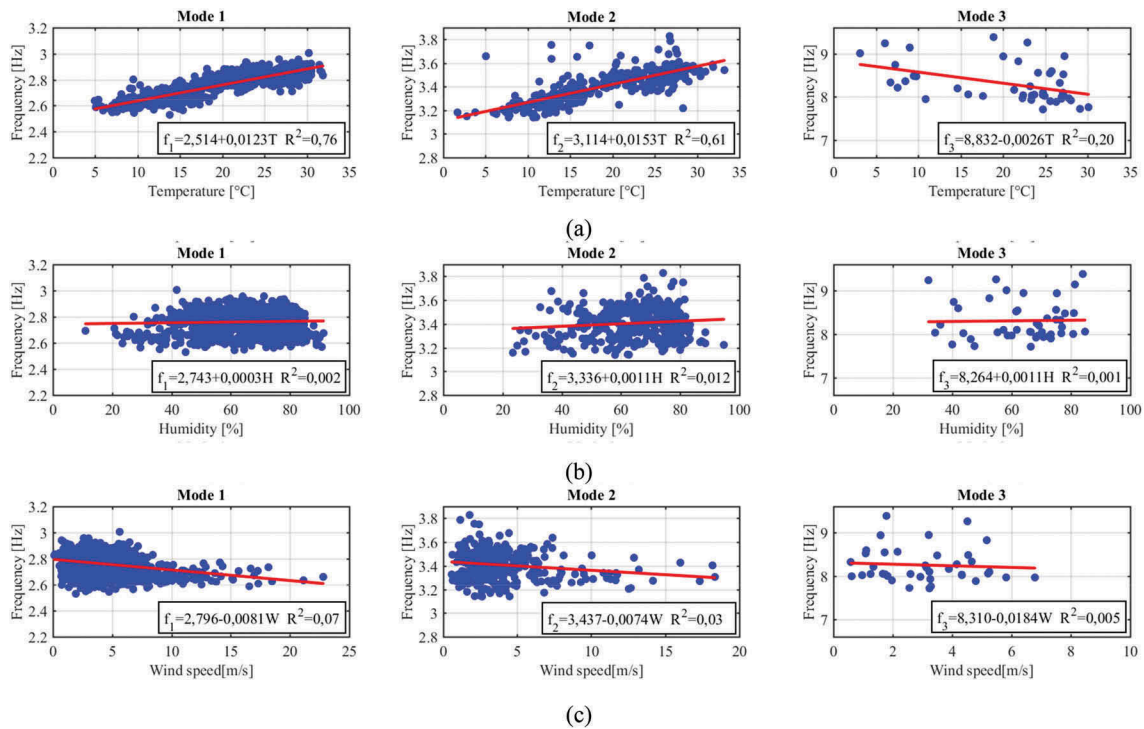


Figure 25. Modal tracking of the identified frequency for each mode.

The variation of humidity seems not to have a significant influence on the tracked modes (Figure 26b). This can be justified with the plastered and painted external surface that limits the water absorption of the walls. The wind speed effect on the natural frequencies (Figure 26c) is low, exhibiting a slighting negative correlation for all the tracked

modes. In Cantieni (2014) it is also observed a decrease of the frequencies in the case of strong wind activity. This phenomenon is justified by the crack openings in the case of strong dynamic actions that produce a reduction of the stiffness. It is worth noting that the first two modes are well identified in a regime of strong wind, but the third is



**Figure 26.** Identified frequencies vs the recorded temperature (a), the recorded humidity (b) and the average wind-speed (c).

not identified anymore. This can be explained by the frequency content of the wind excitation, whose energy tend to be centred in the low frequencies, allowing a better identification of the lowest modes.

The variation of the considered environmental parameters (temperature, humidity and wind speed) during the first 12 months of monitoring is also summarized in Table 6, together with the corresponding variation of the three main frequencies as obtained from the linear regression of the data with respect to the measured environmental effects.

## 6. Conclusive remarks

The paper presented an application of the WSN technology to the long-time monitoring of historic constructions, developed within the research project MOSCARDO. The project was aimed at providing a general framework to: (i)

**Table 6.** Range of variation of the frequencies over the first 12 months of monitoring obtained from the linear regression of the data with respect to the measured environmental effects.

	1st Mode		2nd Mode		3rd Mode	
	Min	Max	Min	Max	Min	Max
Temperature [°C]	4.95	31.90	1.68	33.23	3.130	30.07
Frequency [Hz]	2.638	2.832	3.182	3.541	9.009	7.764
Humidity [%]	11.00	91.33	23.50	94.75	32.00	84.75
Frequency [Hz]	2.693	2.675	3.157	3.223	9.237	8.059
Wind speed [m/s]	0.12	22.81	0.56	18.36	0.58	6.794
Frequency [Hz]	2.826	2.661	3.328	3.307	8.326	7.970

check the structural health of the monitored structures at any time and from any location, and to real-time detect any potential damage that may compromise its habitual use; (ii) provide historical data sets that can be used to permanently monitor the tested structure and to develop predictions (and promptly act for repairing when needed); (iii) gain an in-depth and organic knowledge of the historical construction, from which new models and tools can be developed to simulate the mechanical behavior of the structure. Based on the specific requirements of CHS (use of low-cost sensors and low visual impact of the sensor grid), the design of customized hardware and software technologies has been performed and preliminarily tested on several representative case studies. The system is operating since September 2018 and is able to acquire data continuously. Data recorded by the WSN are in agreement with those acquired during a preliminary test performed with traditional seismic accelerometers, and after an initial period of debugging and adjustment, the system has now gained stability and reliability and is able to acquire data without interruptions. Eventually, an automatic modal identification procedure has been set-up, and the effects of temperature and wind speed on the tower modal properties are in line with the behaviour observed in other studies.

Practitioners and stakeholders, but the public administrations in charge of risk management of CHS also, will benefit from the results of the WSN for SHM here proposed in term of improving prevention and risk awareness. In addition, the scientific community

will benefit of the collected data to improve, f.i., the knowledge of the physical correlation between environmental parameters and modal properties.

## Acknowledgements

The authors kindly acknowledge the Region of Tuscany and the Italian Ministry of Education, Universities, and Research for the financial support of the MOSCARDIO research project (call FAR-FAS 2014).

## Disclosure statement

No potential conflict of interest was reported by the authors.

## ORCID

Paolo Barsocchi  <http://orcid.org/0000-0002-6862-7593>  
 Gianni Bartoli  <http://orcid.org/0000-0002-5536-3269>  
 Michele Betti  <http://orcid.org/0000-0002-8389-3355>  
 Maria Girardi  <http://orcid.org/0000-0002-7358-5607>  
 Daniele Pellegrini  <http://orcid.org/0000-0002-3416-771X>  
 Giacomo Zini  <http://orcid.org/0000-0003-3772-2472>

## References

- Acito, M., M. Bocciarelli, C. Chesi, and G. Milani. 2014. Collapse of the clock tower in Finale Emilia after the May 2012 Emilia Romagna earthquake sequence: Numerical insight. *Engineering Structures* 72:70–91. doi:10.1016/j.engstruct.2014.04.026.
- ANSI (American National Standards Institute). 1990. Vibration of buildings. Guidelines for the measurement of vibrations and evaluation of their effects on buildings. ANSI S2. 47–1990.
- Azzara, R. M., G. De Roeck, M. Girardi, C. Padovani, D. Pellegrini, and E. Reynders. 2018. The influence of environmental parameters on the dynamic behaviour of the San Frediano bell tower in Lucca. *Engineering Structures* 156:175–87. doi:10.1016/j.engstruct.2017.10.045.
- Azzara, R. M., M. Girardi, V. Iafolla, D. M. Lucchesi, C. Padovani, and D. Pellegrini. 2019. Ambient vibrations of age-old masonry towers: Results of long-term dynamic monitoring in the historic centre of Lucca. *International Journal of Architectural Heritage* 1–17. doi:10.1080/15583058.2019.1695155.
- Barlindhaug, S., I. M. Holm-Olsen, and H. Tømmervik. 2007. Monitoring archaeological sites in a changing landscape - Using multitemporal satellite remote sensing as an “early warning” method for detecting regrowth processes. *Archaeological Prospection* 14 (4):231–44. doi:10.1002/arp.307.
- Barsocchi, P., P. Cassara, F. Mavilia, and D. Pellegrini. 2018. Sensing a city’s state of health: Structural monitoring system by internet-of-things wireless sensing devices. *IEEE Consumer Electronics Magazine* 7:22–31. doi:10.1109/MCE.2017.2717198.
- Barsocchi, P., E. Ferro, L. Fortunati, F. Mavilia, and F. Palumbo. 2014. EMS@CNR: An Energy monitoring sensor network infrastructure for in-building location-based services. In Proceedings of the International Conference on High Performance Computing & Simulation (HPCS2014), Bologna, Italy, July 21–25. doi:10.1109/HPCSim.2014.6903779.
- Bartoli, G., M. Betti, L. Galano, and G. Zini. 2019. Numerical insights on the seismic risk of confined masonry towers. *Engineering Structures* 180:713–27. doi:10.1016/j.engstruct.2018.10.001.
- Bartoli, G., M. Betti, and S. Monchetti. 2017. Seismic risk assessment of historic masonry towers: Comparison of four case studies. *Journal of Performance of Constructed Facilities* 31 (5):04017039. doi:10.1061/(ASCE)CF.1943-5509.0001039.
- Brincker, R., and C. E. Ventura. 2015. *Introduction to operational modal analysis*. New York: John Wiley & Sons Inc.
- Cabboi, A., F. Magalhães, C. Gentile, and Á. Cunha. 2017. Automated modal identification and tracking: Application to an iron arch bridge. *Structural Control Health Monitoring* 24:e1854. doi:10.1002/stc.1854.
- Cantieni, R. 2014. One-year monitoring of a historic bell tower. *Key Engineering Materials* 628:73–78. doi:10.4028/www.scientific.net/kem.628.73.
- Cavalagli, N., G. Comanducci, C. Gentile, M. Guidobaldi, A. Saisi, and F. Ubertini. 2017. Detecting earthquake-induced damage in historic masonry towers using continuously monitored dynamic response-only data. *Procedia Engineering* 199:3416–21. doi:10.1016/j.proeng.2017.09.581.
- Cavalagli, N., G. Comanducci, and F. Ubertini. 2018. Earthquake-induced damage detection in a monumental masonry bell-tower using long-term dynamic monitoring data. *Journal of Earthquake Engineering* 22 (1):96–119. doi:10.1080/13632469.2017.1323048.
- Ceravolo, R., E. Matta, A. Quattrone, and L. Zanotti Fragonara. 2017. Amplitude dependence of equivalent modal parameters in monitored buildings during earthquake swarms. *Earthquake Engineering Structural Dynamics* 46 (14):2399–417. doi:10.1002/eqe.2910.
- Cheyne, E., J. B. Jakobsen, and J. Snæbjörnsson. 2016. Buffeting response of a suspension bridge in complex terrain. *Engineering Structures* 128:474–87. doi:10.1016/j.engstruct.2016.09.060.
- Clementi, F., A. Pierdicca, G. Milani, V. Gazzani, M. Poiani, and S. Lenci. 2018. Numerical model upgrading of ancient bell towers monitored with a wired sensors network. In Proceedings of 10th International Masonry Conference (IMC), Milan, Italy, July 9–11.
- Dessi, D., and G. Camerlengo. 2015. Damage identification techniques via modal curvature analysis: Overview and comparison. *Mechanical Systems and Signal Processing* 52–53:181–205. doi:10.1016/j.ymsp.2014.05.031.
- DPCM2011 (Direttiva del Presidente del Consiglio dei Ministri). 2011. Direttiva del Presidente del Consiglio dei Ministri per la valutazione e riduzione del rischio sismico del patrimonio culturale con riferimento alle NTC 2008. G. U. n. 47 del 26.02.2011 (in Italian).
- Gentile, C., M. Guidobaldi, and A. Saisi. 2016. One-year dynamic monitoring of a historic tower: Damage detection under changing environment. *Meccanica* 51 (11):2873–89. doi:10.1007/s11012-016-0482-3.

- Girardi, M., C. Padovani, and D. Pellegrini. 2015. The NOSA-ITACA code for the safety assessment of ancient constructions: A case study in Livorno. *Advances in Engineering Software* 89:64–76. doi:10.1016/j.advengsoft.2015.04.002.
- Girardi, M., C. Padovani, D. Pellegrini, and L. Robol. 2019. Model updating procedure to enhance structural analysis in FE code NOSA-ITACA. *Journal of Performance of Constructed Facilities* 33 (4):04019041. doi:10.1061/(ASCE)CF.1943-5509.0001303.
- Imregun, M., and D. J. Ewins. 1995. Complex modes-origins and limits. In Proceedings of the 13th International Modal Analysis Conference, Nashville, Tennessee, USA, February 13–16, 1995.
- Ivorra, S., F. J. Pallarés, and J. M. Adam. 2009. Experimental and numerical results from the seismic study of a masonry bell tower. *Advances in Structural Engineering* 12 (2):287–93. doi:10.1260/136943309788251641.
- Ljung, L. 1987. *System identification: Theory for user*. New York: Prentice Hall, Englewood Cliffs.
- Magalhães, F., A. Cunha, and E. Caetano. 2009. Online automatic identification of the modal parameters of a long span arch bridge. *Mechanical Systems and Signal Processing* 23:316–29. doi:10.1016/j.ymssp.2008.05.003.
- Magalhães, F., A. Cunha, and E. Caetano. 2012. Vibration based structural health monitoring of an arch bridge: From automated OMA to damage detection. *Mechanical Systems and Signal Processing* 28:212–28. doi:10.1016/j.ymssp.2011.06.011.
- Marwitz, S., and V. Zabel. 2018. Relations between the quality of identified modal parameters and measured data obtained by structural monitoring. In Proceedings of the International Conference on Noise and Vibration Engineering (ISMA2018), Leuven, Belgium, September 17–19.
- Neu, E., F. Janser, A. A. Khatibi, and A. C. Orifici. 2017. Fully automated operational modal analysis using multi-stage clustering. *Mechanical Systems and Signal Processing* 84:308–23. doi:10.1016/j.ymssp.2016.07.031.
- Pecorelli, M. L., R. Ceravolo, and R. Epicoco. 2018. An automatic modal identification procedure for the permanent dynamic monitoring of the sanctuary of vicoforte. *International Journal of Architectural Heritage* 1–15. doi:10.1080/15583058.2018.1554725.
- Peeters, B., and G. De Roeck. 2001. Stochastic system identification for operational modal analysis: A review. *Journal of Dynamic Systems, Measurement, and Control* 123 (4):659–67. doi:10.1115/1.1410370.
- Potenza, F., F. Federici, M. Lepidi, V. Gattulli, F. Graziosi, and A. Colarieti. 2015. Long-term structural monitoring of the damaged Basilica S. Maria di Collemaggio through a low-cost wireless sensor network. *Journal of Civil Structural Health Monitoring* 5:655–76. doi:10.1007/s13349-015-0146-3.
- Rainieri, C., and G. Fabbrocino. 2014. Influence of model order and number of block rows on accuracy and precision of modal parameter estimates in stochastic subspace identification. *International Journal of Lifecycle Performance Engineering* 1 (4):317–34. doi:10.1504/IJLCPE.2014.064099.
- Rainieri, C., and G. Fabbrocino. 2015. Development and validation of an automated operational modal analysis algorithm for vibration-based monitoring and tensile load estimation. *Mechanical Systems and Signal Processing* 60:512–34. doi:10.1016/j.ymssp.2015.01.019.
- Ramos, L. F., L. Marques, P. B. Lourenço, G. De Roeck, A. Campos-Costa, and J. Roque. 2010. Monitoring historical masonry structures with operational modal analysis: Two case studies. *Systems and Signal Processing* 24:1291–305. doi:10.1016/j.ymssp.2010.01.011.
- Reynders, E., J. Houbrechts, and G. De Roeck. 2012. Fully automated (operational) modal analysis. *Mechanical Systems and Signal Processing* 29:228–50. doi:10.1016/j.ymssp.2012.01.007.
- Reynders, E., R. Pintelon, and G. De Roeck. 2008. Uncertainty bounds on modal parameters obtained from stochastic subspace identification. *Mechanical Systems and Signal Processing* 22:948–69. doi:10.1016/j.ymssp.2007.10.009.
- Rizzo, M., M. Betti, O. Spadaccini, and A. Vignoli. 2017. Improvement of structural monitoring of jacket platform. In Proceedings of The Twenty-seventh International Ocean and Polar Engineering Conference (ISOPE2017), San Francisco, CA, June 25–30.
- Salawu, O. S. 1997. Detection of structural damage in frequency: Detection through changes a review. *Engineering Structures* 19 (9):718–23. doi:10.1016/S0141-0296(96)00149-6.
- Shih, C. Y., Y. G. Tsuei, R. J. Allemang, and D. L. Brown. 1988. Complex mode indication function and its applications to spatial domain parameter estimation. *Mechanical Systems and Signal Processing* 2 (4):367–77. doi:10.1016/0888-3270(88)90060-X.
- Sinou, J. J. 2009. A review of damage detection and health monitoring of mechanical systems from changes in the measurement of linear and non-linear vibrations. In *Mechanical vibrations: Measurement, effects and control*, ed. R. C. Sapri, 643–702. New York: Nova Science Publishers.
- SMooHS – Smart Monitoring of Historic Structures7, 2011. EU-FP project. Grant agreement no. 212939, 01-12-2008-30-11-2011. <https://cordis.europa.eu/project/id/212939>.
- Sohn, H., C. R. Farrar, F. M. Hemez, D. D. Shunk, D. W. Stinemat, B. R. Nadler, and J. J. Czarnecki. 2004. A review of structural health monitoring literature : 1996-2001. Report, LA-13976-MS, Los Alamos National Laboratory.
- Ubertini, F., N. Cavalagli, G. Comanducci, A. L. Materazzi, A. L. Pisello, and F. Cotana. 2016. Automated post-earthquake damage detection in a monumental bell tower by continuous dynamic monitoring. In Proceedings of the 10th International Conference on Structural Analysis of Historical Constructions (SAHC2016), Leuven, Belgium, September 13–15.
- Ubertini, F., G. Comanducci, N. Cavalagli, A. L. Pisello, A. L. Materazzi, and F. Cotana. 2017. Environmental effects on natural frequencies of the San Pietro bell tower in Perugia, Italy, and their removal for structural performance assessment. *Mechanical Systems and Signal Processing* 82:307–22. doi:10.1016/j.ymssp.2016.05.025.
- Ubertini, F., C. Gentile, and A. L. Materazzi. 2013. Automated modal identification in operational conditions and its application to bridges. *Engineering Structures* 46:264–78. doi:10.1016/j.engstruct.2012.07.031.
- Van Overschee, P., and B. De Moor. 1996. *Subspace identification for linear systems. Theory-implementation-applications*. New York: Kluwer Academic Publishers. doi:10.1007/978-1-4613-0465-4.

- Verboven, P., E. Parloo, P. Guillaume, and M. Van Overmeire. 2002. Autonomous structural health monitoring-part I: Modal parameter estimation and tracking. *Mechanical Systems and Signal Processing* 16 (4):637–57. doi:10.1006/mssp.1492.
- Wu, W. H., S. W. Wang, C. C. Chen, and G. Lai. 2017. Assessment of environmental and nondestructive earthquake effects on modal parameters of an office building based on long-term vibration measurements. *Smart Materials and Structures* 26 (5):055034. doi:10.1088/1361-665X/aa6ae6.
- Zini, G., M. Betti, G. Bartoli, and S. Chiostrini. 2018. Frequency vs time domain identification of heritage structures. *Procedia Structural Integrity* 11:460–69. doi:10.1016/j.prostr.2018.11.115.
- Zonta, D., M. Pozzi, and P. Zanon. 2008. Managing the historical heritage using distributed technologies. *International Journal of Architectural Heritage* 2 (3):200–25. doi:10.1080/15583050802063691.
- Zonta, D., H. Wu, M. Pozzi, P. Zanon, M. Ceriotti, L. Mottola, G. P. Picco, A. L. Murphy, S. Guna, and M. Corra. 2010. Wireless sensor networks for permanent health monitoring of historic buildings. *Smart Structures and Systems* 6 (5):595–618. doi:10.12989/sss.2010.6.5\_6.595.